

---

---

# Toward Efficient In Situ Microphone Calibration Procedures Using Laser-Induced Plasma

Máté Szóke (Virginia Tech),  
Christopher J. Bahr (NASA Langley),  
Louis Cattafesta (Florida State University),  
Karl-Stéphane Rossignol (DLR),  
Yang Zhang (Florida State University)

---

---

28th AIAA/CEAS Aeroacoustics Conference (Southampton, UK)  
4th Hybrid Anechoic Wind Tunnel Workshop  
June 15, 2022

# Contents

**Introduction** to laser-induced plasma

**Aims**

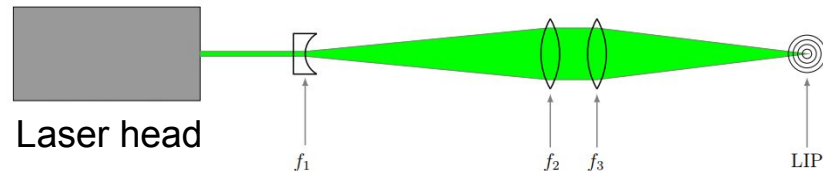
**Overview** of collaborators and facilities

Assessment of **laser power** and its effects

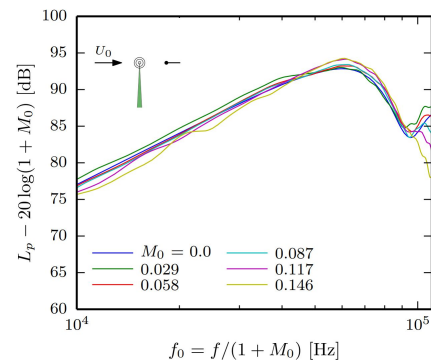
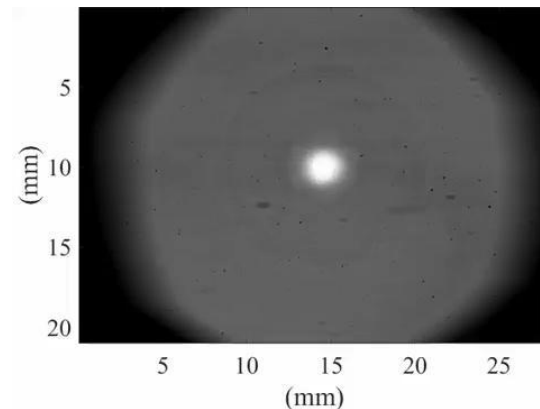
Assessment of **microphone responses** and their impact

**Conclusions** and future directions

# Overview, aims



- **Properties** of laser-induced plasma (**LIP**):
  - **Tight-focusing of laser beam** results in plasma formation once a sufficiently **high energy density** ( $W/m^2$ ) is reached
  - Generates a **deterministic acoustic source**
  - Well localized, repeatable, nonintrusive
  - **Short duration** allows propagation path identification in noisy and reflective environments
  - **Omnidirectional** about beam axis (no flow)
  - Flow introduces **convection effect**  
**Can be accounted for**, see AIAA-2015-3146
  - **Suitable for high-frequency analysis**  
(2-100 kHz) + good signal-to-noise ratio (loud)
- Signal bandwidth is greater than most acoustic instrumentation (**wideband excitation**)
- Observed **waveform depends on instrumentation**:  
*potentially indicating microphone self-scattering effects:*  
*Aim: Can we obtain a correction?*



# Acoustic signature

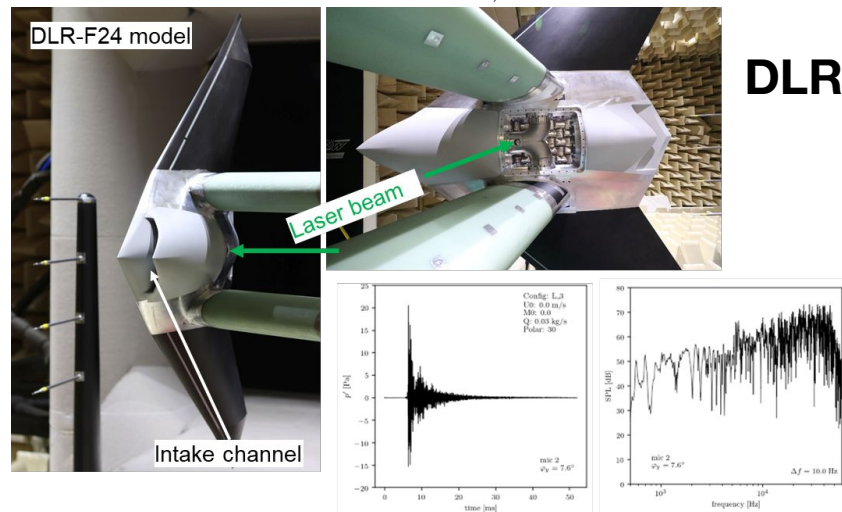
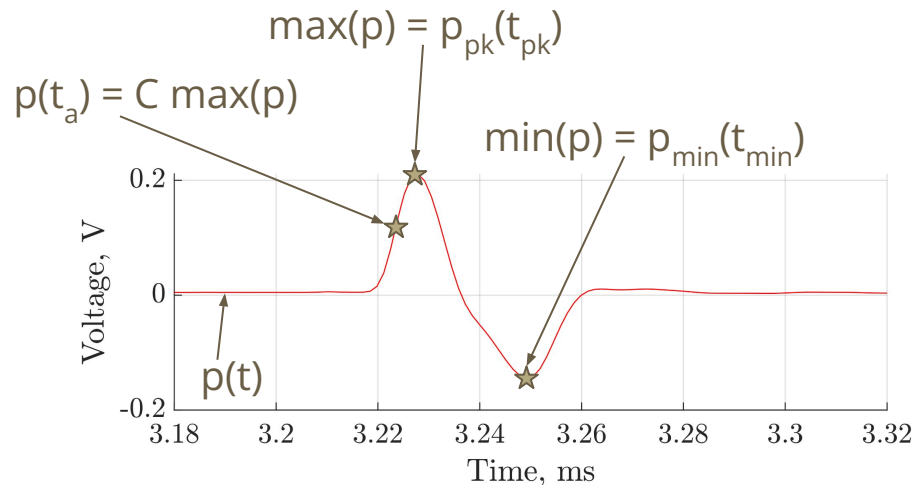
The LIP produces a repeatable, deterministic, **short acoustic waveform**.

We identify the **following key properties**:

- **Arrival time ( $t_a$ )** at a given percentage of the peak pressure value (e.g.,  $C = 50\%$ ), measured from reference signal (Q-switch, photodetector)
- **Peak pressure** or max. pressure ( $p_{pk}$ )
- **Negative peak** pressure or min. pressure ( $p_{min}$ )
- **Time span** (arrival time to min. pressure)

Some **examples** of LIP use:

- **Shear layer refraction** assessment (AIAA-2015-2976, AIAA-2018-3118, AIAA-2020-1253, etc.)
- **Duct mode excitation** (see right, AIAA-2022-XXXX)
- Acoustic **noise shielding** (AIAA-2017-3195, AIAA-2018-2820, AIAA-2018-2821)



# Contents

**Introduction** to laser-induced plasma

**Aims**

**Overview** of collaborators and facilities

Assessment of **laser power** and its effects

Assessment of **microphone responses** and their impact

**Conclusions** and future directions

# Instrumentation

## Examples of instrumentation used at the collaborating facilities

As a general rule-of-thumb for desired sampling rate:

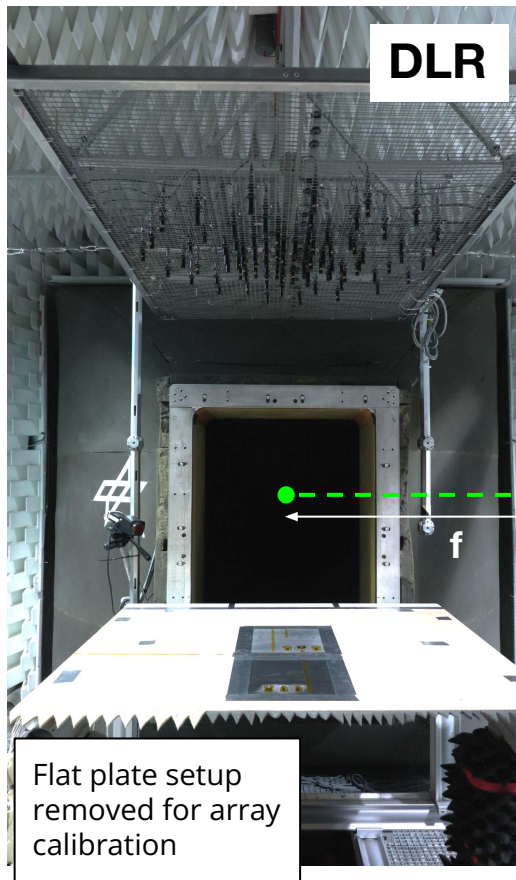
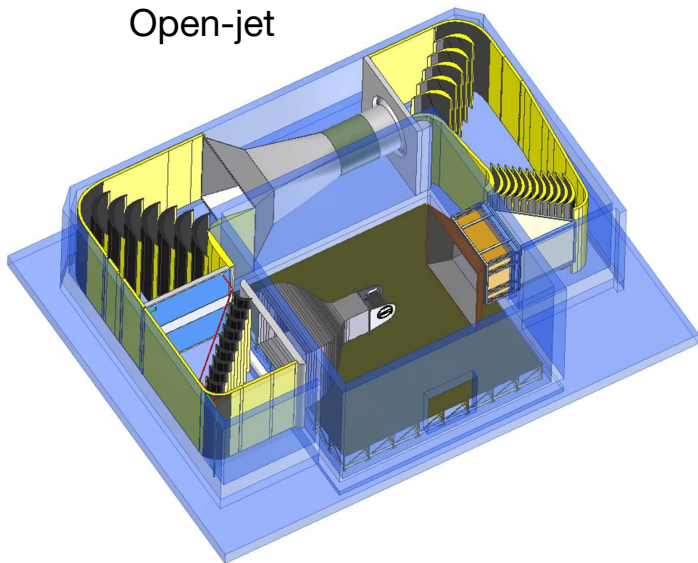
- Frequency domain investigation: **2.5x the largest frequency of interest** (e.g., for 20 kHz use 50+ kS/s)
- Time-domain investigation, **10x the smallest time-scale of interest** (e.g., time-span of LIP)

INSTRUMENTATION	VT SWT	NASA Langley OFF	DLR (AWB)	FSU
Microphones used	GRAS 46BD-FV (5 Hz - 70 kHz) B&K 4138 (6.5 Hz - 140 kHz);	B&K 4138 (6.5 Hz - 140 kHz); B&K 4938 (4 Hz - 70 kHz)	GRAS 48 LX-1 (10 Hz - 70 kHz) LinearX M51 (20 Hz - 40 kHz)	GRAS 40BE (4 Hz - 80 kHz); B&K 4958 (10 Hz - 20 kHz)
DAQ system	General Standards Corp. PMC66-18AI64SSC750K (+ <b>Oscilloscope</b> )	NI PXIe 4480	GBM Viper 48 Channels (3X)	NI PXI-1045; NI PXI-4462
Sampling rate	748.8 kS/s	1.25 MS/s	250 kS/s 500 kS/s (10 channels)	204.8 kS/s
Laser emission detection	Photodetector signal	Photodetector signal, Q-switch	Q-switch	Photodetector signal
Filters	Low-pass 150 kHz	Built-in anti alias, Variable analog conditioning	Built-in anti alias	Low-pass 80 kHz
Flow speed range	0-75 m/s	0-58 m/s	0-65 m/s	0-70 m/s
LIP to observer distance	0.9 m	variable within several meters	variable within several meters	< 2 m

# Facilities I.

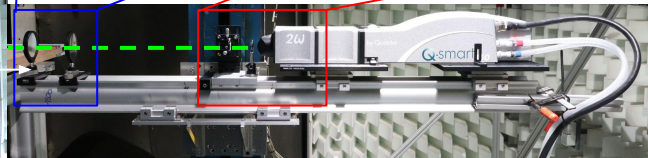
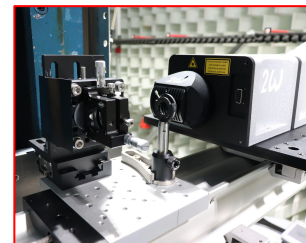
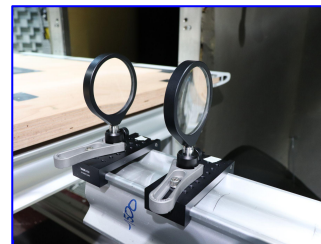
Facility: **AWB**  
2.6' x 3.9' x 9.8'  
(0.8 m x 1.2 m x 3.0 m)  
 $f \approx 500$  mm

Open-jet



$f=+1000$  mm and  
 $f=+500$  mm  
(plano-convex)

$f=-50$  mm  
(bi-concave)



- Quantel Q-Smart 450 Laser (*new*)
- 220 mJ per Pulse (**measured**)
- Beamwidth  $\sim 6.5$  mm
- Pulsewidth  $\sim 5$  ns
- Wavelength: 532 nm

# Facilities II.

Semi-anechoic:  
Kevlar + Hard wall

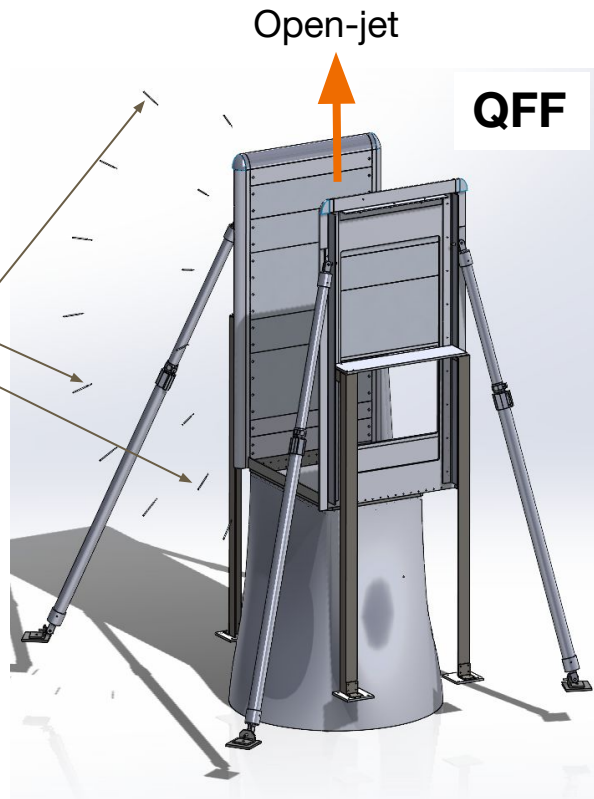


SWT

6' x 6' x 24'  
(1.83 m x 1.83 m x 7.3 m)  
f = 1200 mm

Microphone  
array

Microphones  
90 deg polar  
0 and 30 deg  
azimuth



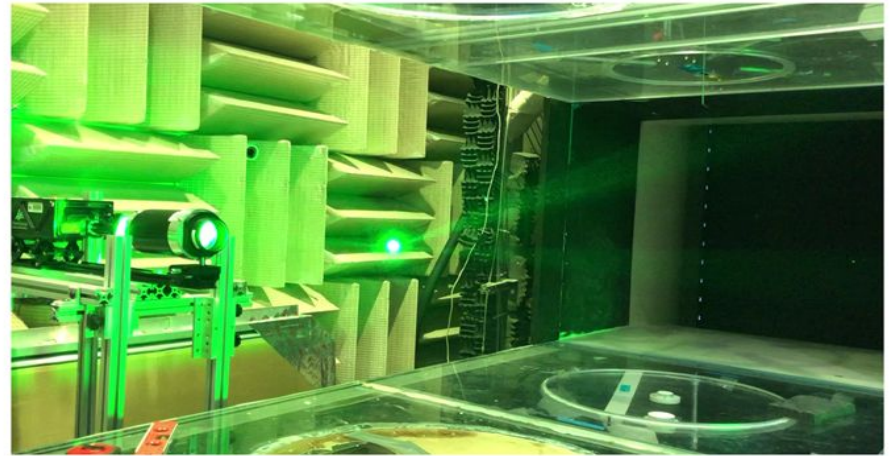
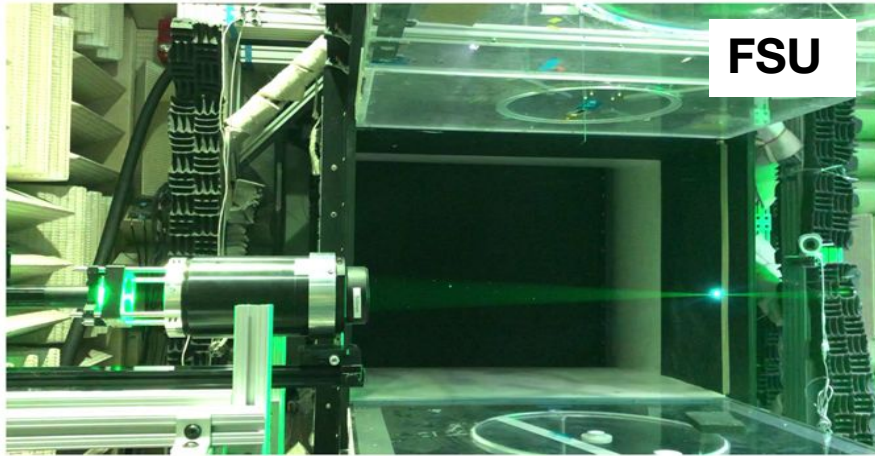
Open-jet

QFF

2' x 3' x 6'  
(0.6 m x 0.91 m x 1.83 m)  
f = 500 mm



# Facilities III.



3' x 4' x 10'  
(0.91 m x 1.22 m x 3 m)  
f = 500 mm  
Kevlar walls

# Collaborators and facilities: Summary

LIP-based experiments	VT SWT	NASA Langley QFF	DLR (AWB)	FSU
Test section size (ft & m)	6' x 6' x 24' 1.83 m x 1.83 m x 7.3 m	2' x 3' x 6' 0.6 m x 0.91 m x 1.83 m	2.6' x 3.9' x 9.8' 0.8 m x 1.2 m x 3.0 m	3' x 4' x 10' 0.91 m x 1.22 m x 3 m
Flow speed range	20 - 75 m/s	0 - 58 m/s	0 - 65 m/s	0 - 70 m/s
Typical test object size (e.g., chord)	0.6 - 0.9 m	0.2 - 0.5 m	0.2 - 0.5 m	0.2 - 0.5 m
Observer angles: polar (defined wrt. Mach vector)	40-140 deg	45-135 deg	~ +/- 180 deg	
Observer angles: azimuth	~ +/- 30 deg	~ +/- 30 deg	~ +/- 60 deg	
Tunnel type(s):	Kevlar walls, Hard walls, Combined (semi-anechoic)	Open-jet, Kevlar panel	Open-jet	Open-jet, Kevlar panel, glass panel

# Contents

**Introduction** to laser-induced plasma

**Aims**

**Overview** of collaborators and facilities

Assessment of **laser power** and its effects

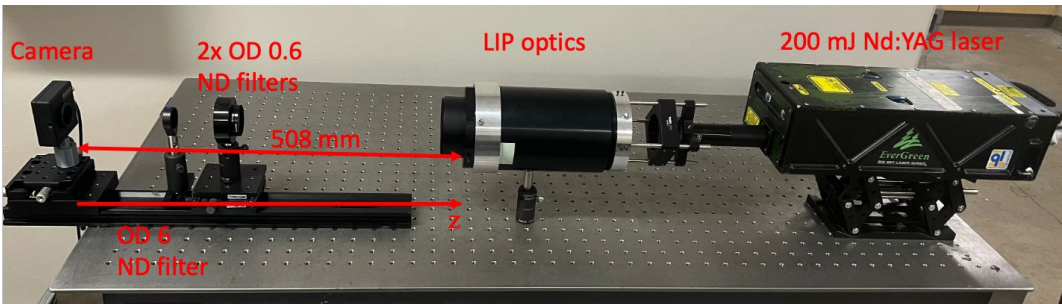
Assessment of **microphone responses** and their impact

**Conclusions** and future directions

# Beam profile measurement: Width from intensity

WinCam UCD12

FSU



**ISO-11146: international standard definition for beam width**

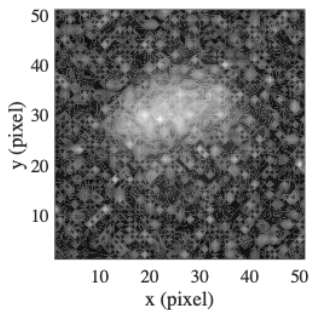
$D_{4\sigma}$  : second-moment width defined as 4x standard deviation ( $\sigma$ ) of intensity

$$4\sigma_x = 4\sqrt{\frac{\int_{-\infty}^{\infty} \int_{-\infty}^{\infty} I(x,y)(x - \bar{x})^2 dx dy}{\int_{-\infty}^{\infty} \int_{-\infty}^{\infty} I(x,y) dx dy}}$$

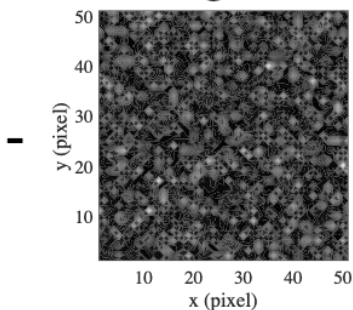
$$\bar{x} = \frac{\int_{-\infty}^{\infty} \int_{-\infty}^{\infty} I(x,y)x dx dy}{\int_{-\infty}^{\infty} \int_{-\infty}^{\infty} I(x,y) dx dy}$$

Beam profile intensity,  $I(x,y)$ , sample at a location near the focal point

raw

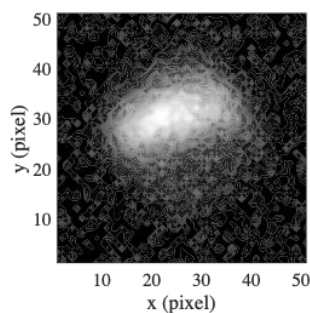


background

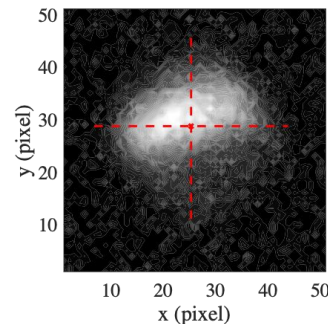


=

de-noised

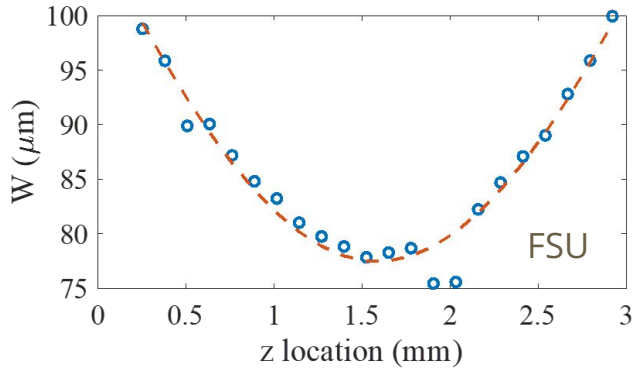


Centroid and second moment width



# Determine energy density from measurements

Beam half width ( $W = D_{4\sigma} / 2$ ) along its axis



**Curve fitting** to measured **W values** using

Beam propagation ratio:  $M^2=21.32$

Beam radius at focal point  $W_0=77 \mu\text{m}$

Location of focal point  $z_0=1.6 \text{ mm}$

$$W^2(z) = W_0^2 + M^4 \left( \frac{\lambda}{\pi W_0} \right)^2 (z - z_0)^2$$

**Calculate energy density (ED) after measuring laser power using an Apollo Laser Alc calorimeter**

Evergreen laser has 20 levels, we decrease level until we obtain LIP at 50% of laser emissions at 2/second repetition rate:

Level 13, < 50% successful sparks

Level 14, > 50% successful sparks

$E_{\text{measured}} = 127 \text{ mJ}$  per pulse at level 14

pulse duration from calorimeter:  $\Delta\tau = 7 \text{ ns}$

$$A_{\text{focal}} = \pi W_0^2$$

**Corresponding ED is considered the formation threshold:**

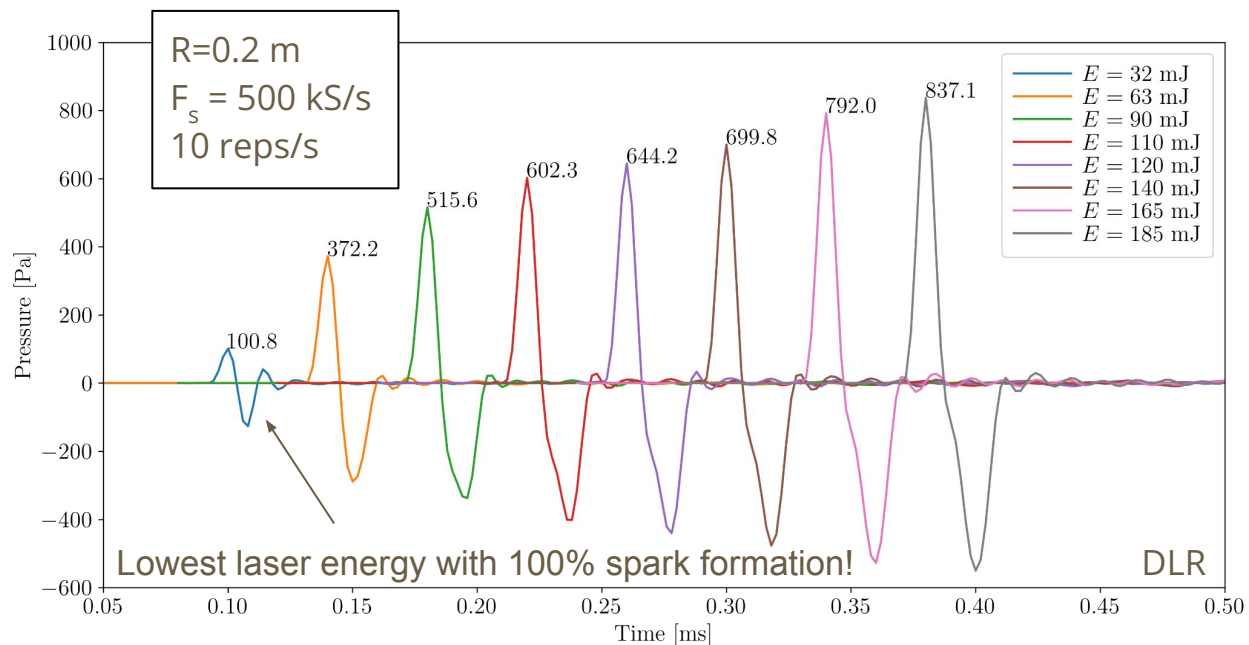
$$ED = \frac{E_{\text{measured}}}{\Delta\tau A_{\text{focal}}} = \frac{127 \text{ mJ}}{7 \text{ ns} \cdot 4.65 \cdot 10^{-5} \text{ cm}^2} = 3.9 \cdot 10^{11} \text{ W/cm}^2$$

Using the calculation of ED as described in appendix, we obtain a very similar value. The remaining unknown in optics-based calculation is  $M^2$ .

# Effect of laser energy on acoustic signature I.

**Varying** and also measuring **laser energy** while capturing sound signature.

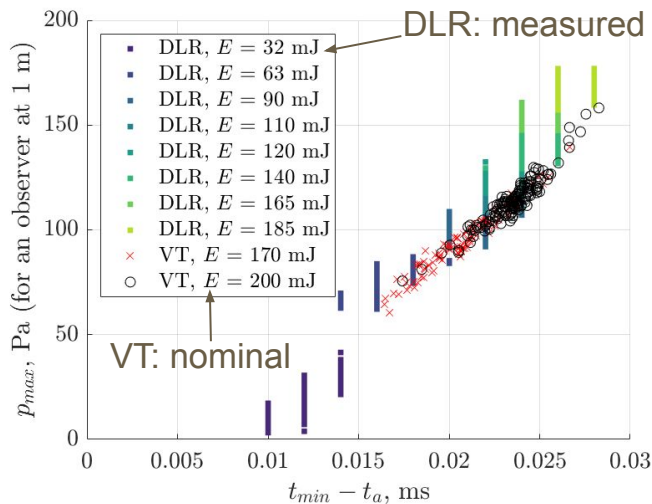
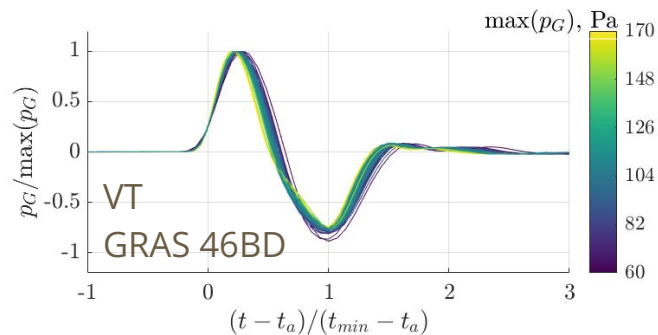
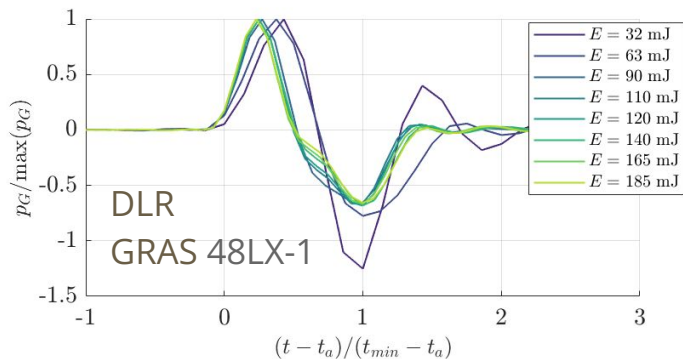
**Waveform mostly independent of laser energy setting**, except at the lowest energy setting.



Brand new laser head (see appendix), **calculation confirms LIP formation for all E values** due to the low  $M^2=2$  value.

# Effect of laser energy on acoustic signature II.

**Good collapse** in **both time** and frequency (not shown) domain when scaled using max pressure and timespan of pulse width. Time span and amplitude are **well correlated**.



**Consistent acoustic characteristics and constant correlation coefficient for a given microphone across the entire range of laser energy levels tested (32 mJ - 200 mJ)**

# Contents

**Introduction** to laser-induced plasma

**Aims**

**Overview** of collaborators and facilities

Assessment of **laser power** and its effects

Assessment of **microphone responses** and their impact

**Conclusions** and future directions



# Microphone calibration approach

Idea and **approach**: processing steps

Effect of microphone configurations: **time and frequency domain**

Microphone **configurations assessed**:

- Effect of **gridcap**
  - GRAS 46BD-FV (VT), 1/4" microphone
  - Bruel and Kjaer 4138 (NASA), 1/8" microphone
- Effect of **flush-mounting behind a wire mesh**
  - GRAS 46BD-FV (VT) 1/4" microphone
- Effect of **pinhole** cap
  - Bruel and Kjaer 4138 (VT), 1/8" microphone

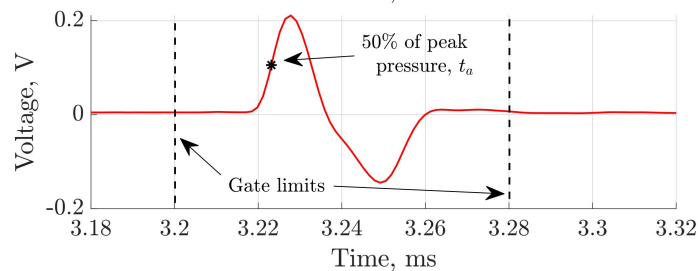
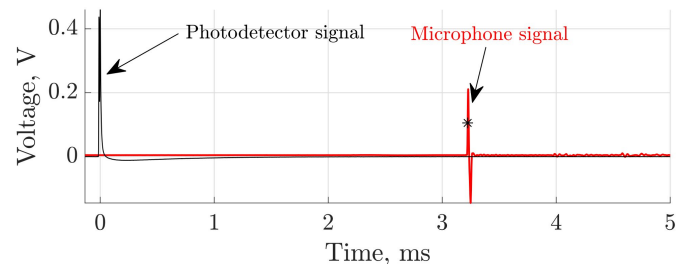
# Calibration approach

**Idea:** Use a reference microphone and observe LIP simultaneously with a microphone that is to be calibrated.

**For each LIP emission:**

- 1) Identify **laser emission time** (Q-switch, photodetector), decide if LIP was formed; **Create blocks** with  $t = 0$  s corresponding to laser emission time.
- 2) Identify: **peak pressure** ( $p(t_{pk})=p_{pk}$ ), pulse **arrival time** ( $t_a$  at 50% of positive peak)
- 3) **Gate signal** ( $p_G$ ) with respect to peak pressure, zero pad to desired block length then calculate Fourier transform.
- 4) Calculate **relative transfer function** from ratio of FFT results ( $T_i$ ), then amplitude ( $S$ ) and phase ( $\varphi$ ) responses
- 5) Corrections:  
**Distance** (obtained from arrival times),  
**Phase:** perform in frequency domain using time-domain information.

Then **average over LIP emissions** to obtain **ensemble-average**



$$T_i = \frac{FFT(p_{G,i})}{FFT(p_{ref})}$$

$$S = 20 \log_{10} |T_i|$$

$$\varphi = \text{atan} \left( \frac{\text{Im}(T_i)}{\text{Re}(T_i)} \right)$$

$$\tau = (t_a - t_{pk})_i - (t_a - t_{pk})_{ref}$$

# Effect of microphone configuration on response I.

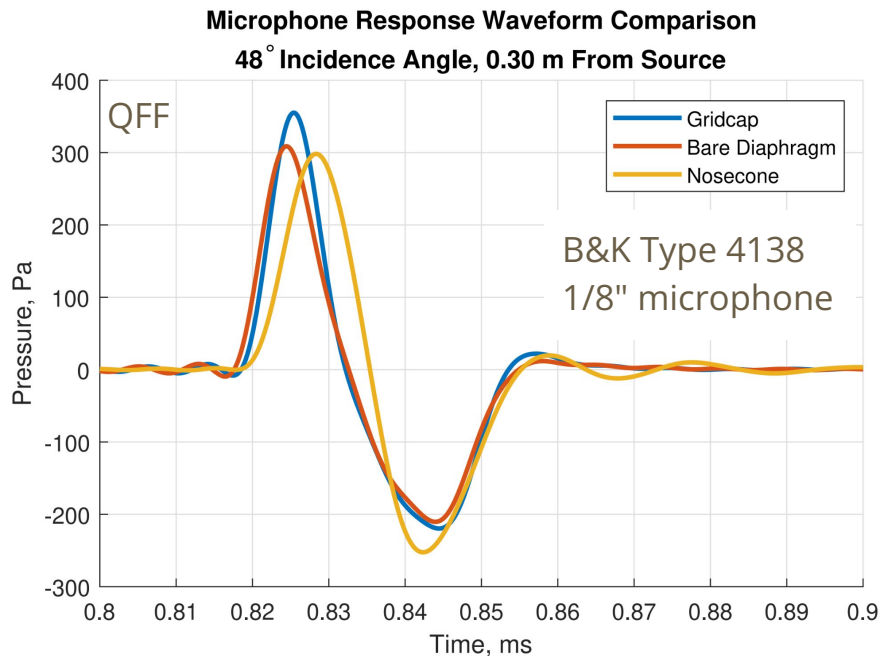
Various microphone configurations show a different waveform when observing near-identical LIP sound signature: **indication of microphone self-scattering**

A commonly known example is the **pinhole microphone response** but the changes in responses shown here are less commonly available, hence **challenging to correct**

We assume that the bare diaphragm configuration has a **broadband 0 dB ("true") response. This is altered when using gridcap, nose cone, etc., configurations**

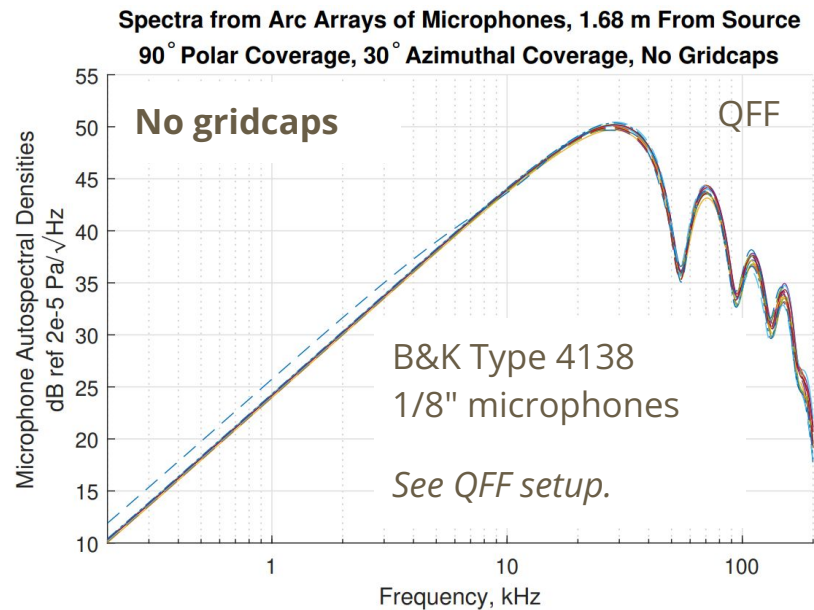
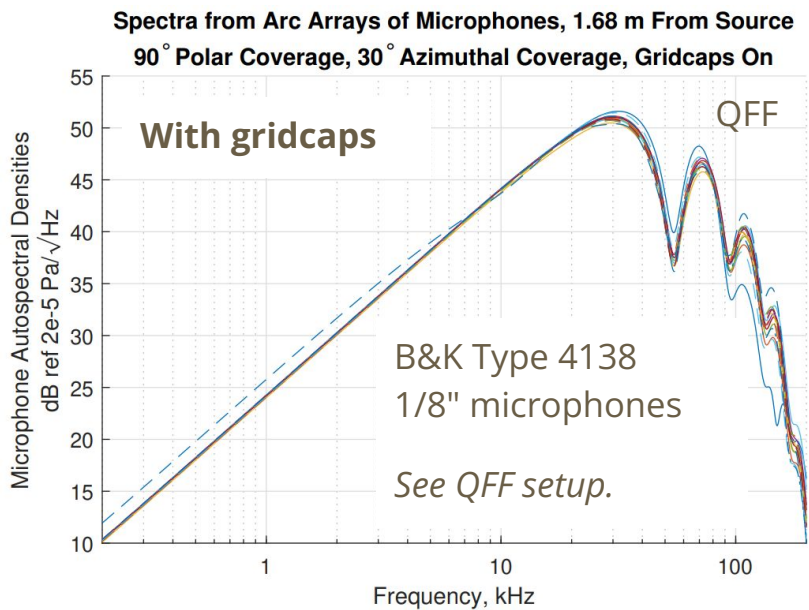
**Response in nose cone** configuration is highly **shape dependent** (variations of nose cones are not shown)

Also an indication that acoustic measurements are **intrusive**



# Effect of microphone configuration on response II.

Variation of autospectral densities. **Gridcap vs. no gridcap**: impacts microphone responses significantly. **No gridcap setup shows** least variability for the instrumentation, best suited to assess **omnidirectionality**

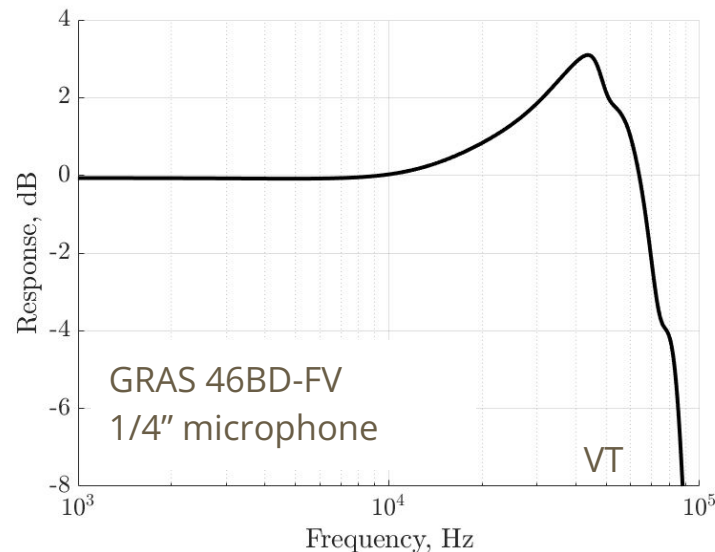
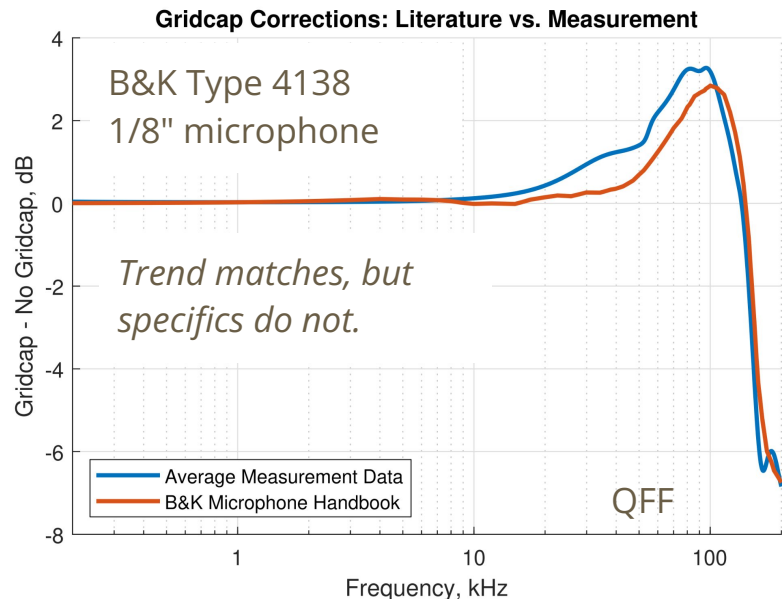


# Effect of gridcap: self-scattering within the capsule

Calculated using LIP and identical microphone as reference.

**Adding a gridcap causes the microphones to respond differently, particularly above 10 kHz.**

**Correction is needed and can be obtained using LIP** and the proposed procedures. Similar procedures could be performed for the nosecone configuration, too.

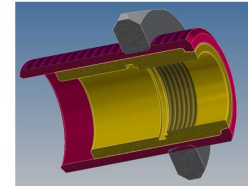
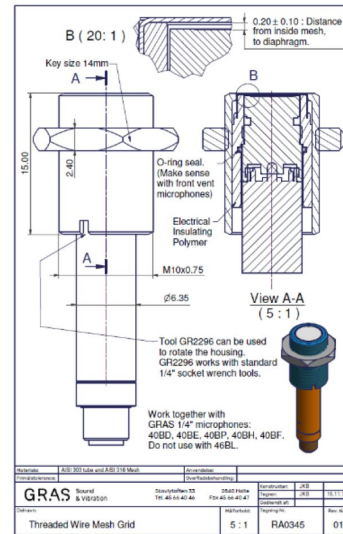
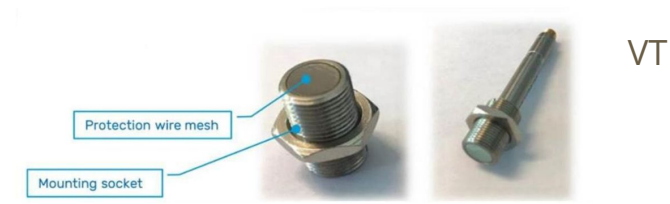


# Flush mounting behind wire mesh I.

Individually mounting GRAS 46BD-FV (1/4") microphones **behind a steel mesh (GRAS RA0345).**

Using a **GRAS 46BD-FV microphone, bare sensor** flush-mounted (without mesh) as the **reference** microphone.

The resulting amplitude and phase response data are to be used for **improving beamformer output** of VT's new 120-element array (see AIAA-2022-XXXX).



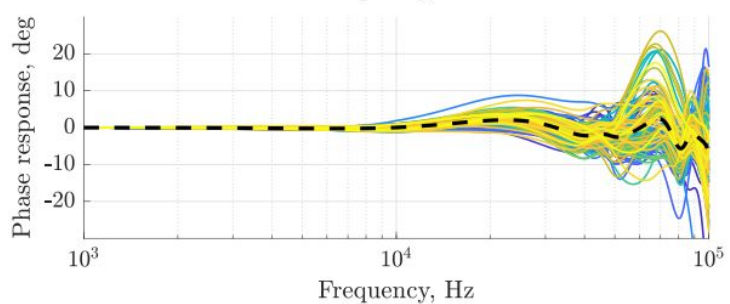
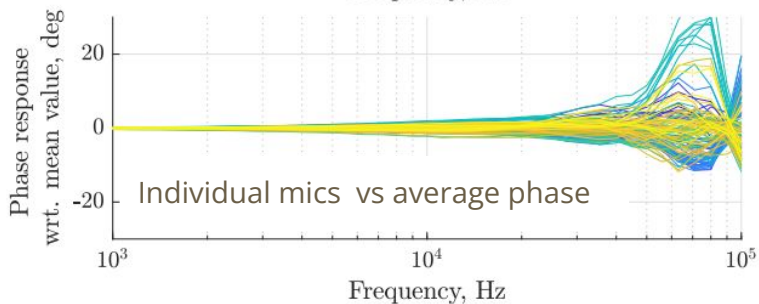
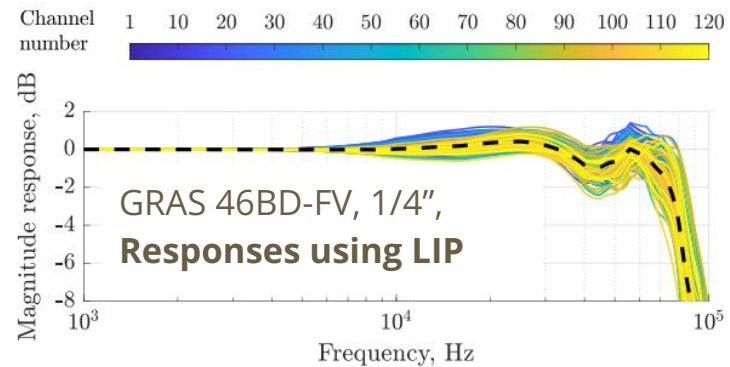
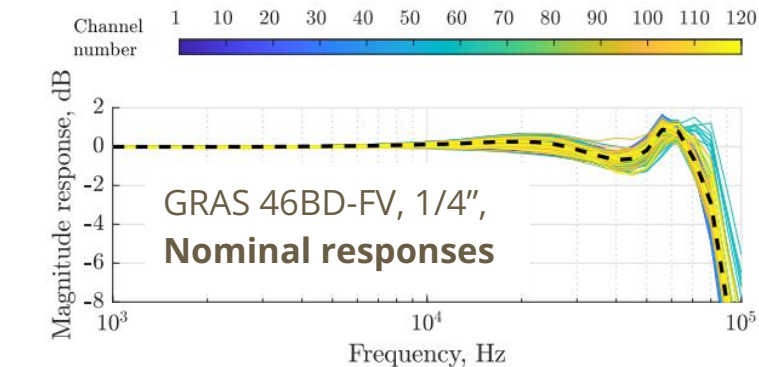
# Flush mounting behind wire mesh II.

VT

The mounts have **minor impact** on response curves

The phase response behaves similarly to the nominal data. Spread is low and comparable until 50 kHz and remains +/- 30 deg afterward

**Correction of mounting effects is now possible**

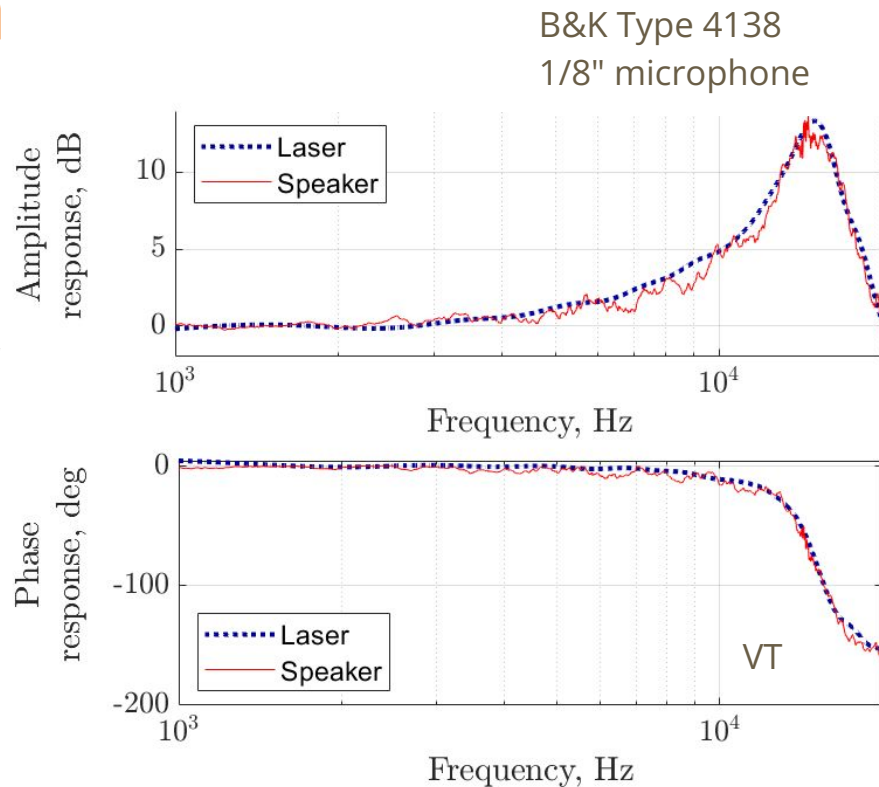
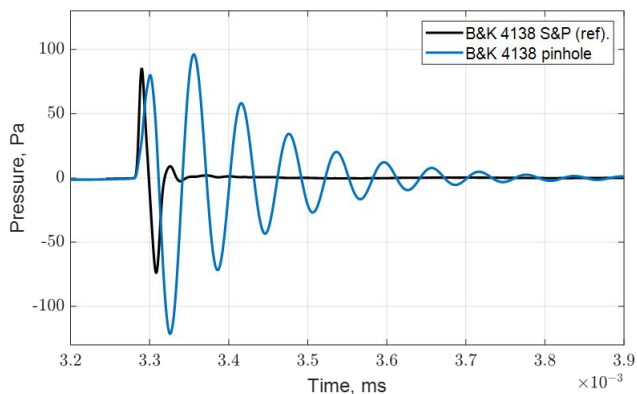


# Effect of pinhole configuration

Calibrating **flush-mounted pinhole microphones** at high-frequencies **using another flush-mounted microphone as a reference** (grid cap) microphone.

**First** method: Using **LIP**. **Second** method: Using a **loudspeaker**, both in an anechoic chamber.

*Both approaches provide similar data but LIP-based data seem to have lower uncertainty.*



*Speaker-based response was obtained by Shishir Damani & Shreyas Chaware*



# Conclusions

- **Acoustic characteristics of LIP** seem to be well scalable and **consistent across a wide range of laser energy levels.**
- **Microphone response changes** when **gridcap, mesh, nose cone, or pinhole** is installed. Using the LIP can reveal these effects.
- **LIP-based calibration procedure reveals microphone self-scattering effects, which could not be corrected before. When uncorrected,** the output of the microphone (array) is greater.
- The deterministic nature of the LIP signal is particularly important in revealing **individual microphone discrepancies**, i.e., helpful for “shakedown” testing.
- LIP offers frequency response calculation in a **nonintrusive** manner (as opposed to electrostatic actuator) while it offers solution for **in situ** calibration as well.
- LIP offers time efficient approach to assess these effects in the facility. It offers an impression on microphone array performance, and can be used to reveal changes over time, i.e., it is a step toward **acoustic uncertainty quantification.**

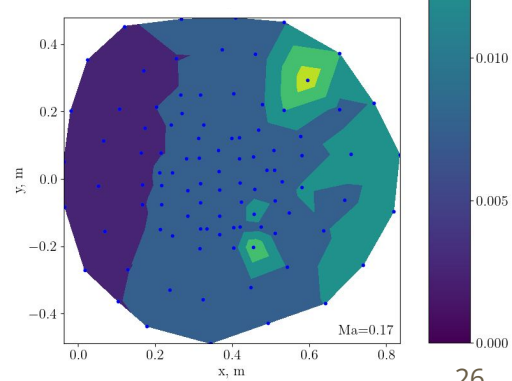
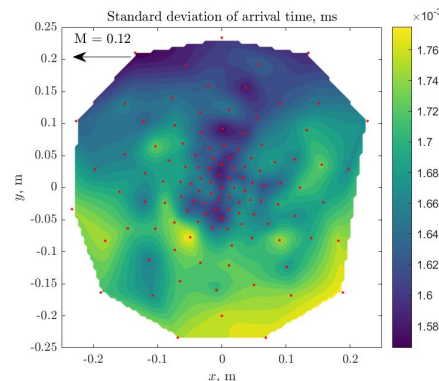
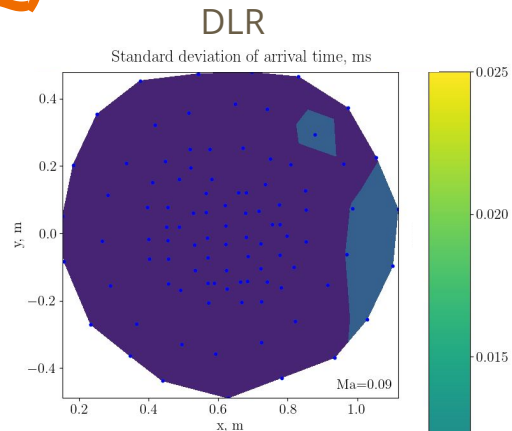
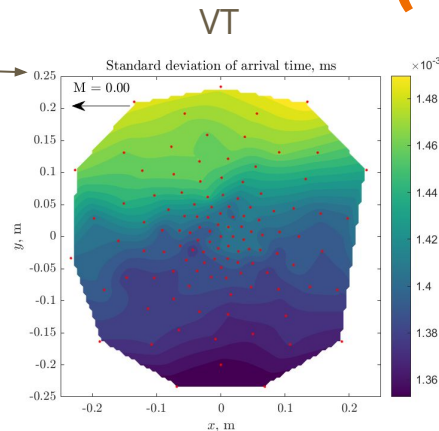
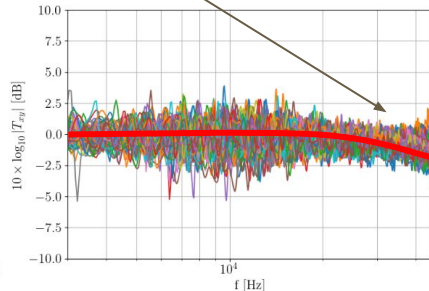
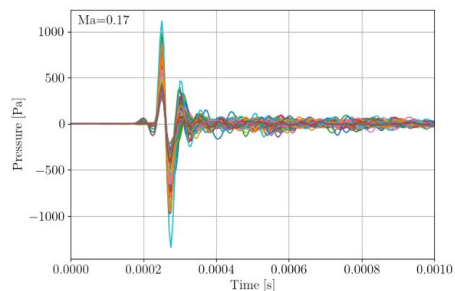
# Future work: Uncertainty quantification (UQ)

Using the **standard deviation of arrival time** to:

- Quantify **uncertainty**
- Assess/**model turbulence scattering effects**
- Can help **quantify instrumentation limitations**, installation irregularities and anomalies

Use **transfer function** to:

- **calibrate beamforming array**, assess **UQ**
- assess **turbulent scattering**



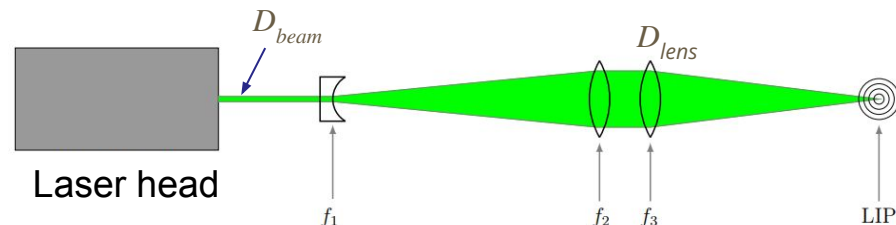
**Thank you for your attention!**

**Questions?**

# Appendix

# Laser-optical design

- Using a **beam expander** plus **focusing optics**
- **Laser properties:** energy per pulse, pulse width (ns), beam: diameter ( $D_{beam}$ ), area, divergence (mrad), wavelength ( $\lambda$ ).
- Determine focusing optics from WTL test section size ( $f_3$ )
- Calculate **magnifying power** (MP) to select beam expander: image lens focal length ( $f_1$ )
- Calculate "**spot size**" ( $\phi_{spot}$ )
- **Diffraction, and aberration limits** (use aspherical lens)
- Minimize  $f_3/D_{lens}$  (i.e., **f-number**) for tight-focusing
- **Assume laser beam quality value** ( $M^2$ )
- Calculate **energy density** in spot
- Exceed threshold\* of  $3.5 \cdot 10^{16} \text{ W/m}^2$

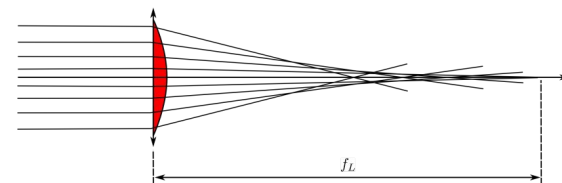


$$MP = \frac{D_{beam}}{D_{lens}} = -\frac{f_2}{f_1} \rightarrow f_1 = -\frac{f_2}{MP}$$

$$\phi_{Spot \text{ Size}} = \phi_{\text{Diffraction}} + \phi_{\text{Aberration}} = \frac{4\lambda M^2 f}{\pi D} + \frac{kD^3}{f^2}$$

<https://www.edmundoptics.com/knowledge-center/application-notes/lasers/beam-expanders/>

Primary limitation: spherical aberration  
 $\sim O(1)$  greater than diffraction (VT, DLR)



\*Phuoc, T.X.: Laser spark ignition: experimental determination of laser-induced breakdown thresholds of combustion gases. Opt. Commun. 175(4), 419–423 (2000)

# Laser-optical arrangements

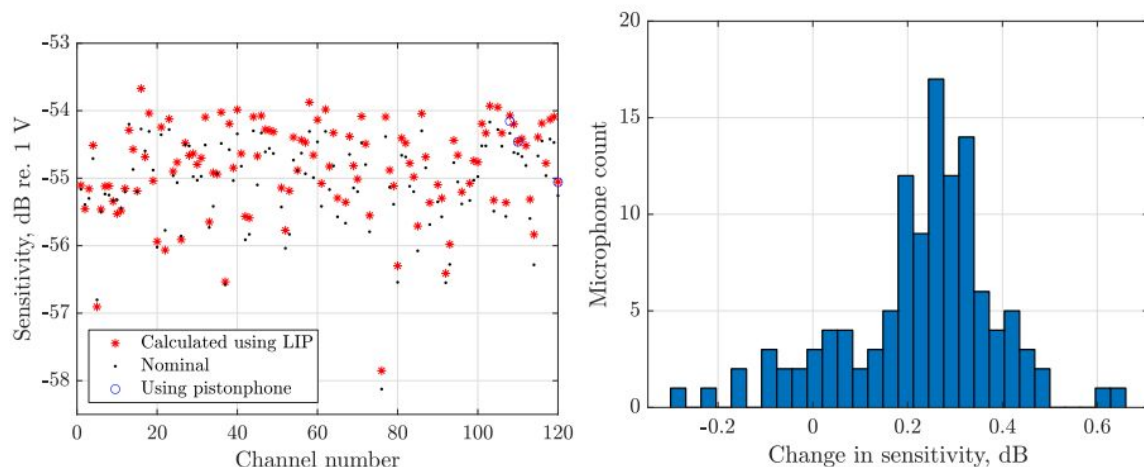
OPTICAL/PLASMA PROPERTIES	VT SWT	NASA Langley QFF	DLR (AWB)	FSU
Focal length	1200 mm	~500 mm (approx.)	1000 mm	500 mm
Laser head	Quantel Evergreen 200	New Wave Gemini	Quantel Q-Smart 450	Quantel Evergreen 200
Laser energy ( $E_L$ )	200 mJ	120 mJ	185 mJ	200 mJ
Laser pulse width	10 ns	3-5 ns	5 ns	10 ns
Laser stability (% RMS)	2%	3.5%	4%	2%
Wavelength	532 nm	532 nm	532 nm	532 nm
Beam diameter (nominal)	6.35 mm	5 mm	6.5 mm	6.5 mm
Laser repetition rate used	5/second	5-10/second	10/second	2/second
Calculated beam energy density at focal point ( $W/cm^2$ )	1.70E12	N/A	4.6E11-2.6E12	3.4E12
Optical setup expenses	\$3000 - 2 pcs of Celestron AVX 6" telescopes (2x\$1500) \$200 - hardware \$1200 - smaller optics (f=200 mm)	\$3500 - lenses and lens holders \$160 - photodetector \$550 - glass panel for use in QFF sidewall	\$1200	\$920 - beam expander (\$600) + converging lens (\$120) + hardware (\$200) + Dantec beam expander (cost unknown)
M <sup>2</sup> number used	20	N/A	2	6
front lens f number	8		10	4

# 1/4" microphones (VT)

*Sensitivity calculation using LIP:* Calculate average  $T_i$  at low frequencies (1 kHz - 2 kHz): provides the difference in microphone sensitivities. Once knowing the sensitivity of the reference sensor, we can calculate the sensitivity of the calibrated microphone.

Comparison against pistonphone calculation: discrepancy is less than 0.1 dB (0.04 and 0.08 dB).

Average change in sensitivity was 0.26 dB with a standard deviation of 0.16 dB.



# 1/8" microphones (QFF)

Effect of gridcap and nose cone on a B&K 4138 microphone: frequency domain

